



Optimal Integration of Offshore Wind Power for a Steadier, Environmentally Friendlier, Supply of Electricity in China

Citation

Lu, Xi, Michael B. McElroy, Chris P. Nielsen, Xinyu Chen, and Junling Huang. 2013. Optimal integration of offshore wind power for a steadier, environmentally friendlier, supply of electricity in China. *Energy Policy* 62:131–138.

Published Version

10.1016/j.enpol.2013.05.106

Permanent link

<http://nrs.harvard.edu/urn-3:HUL.InstRepos:11829293>

Terms of Use

This article was downloaded from Harvard University's DASH repository, and is made available under the terms and conditions applicable to Open Access Policy Articles, as set forth at <http://nrs.harvard.edu/urn-3:HUL.InstRepos:dash.current.terms-of-use#OAP>

Share Your Story

The Harvard community has made this article openly available.
Please share how this access benefits you. [Submit a story](#).

[Accessibility](#)

Optimal Integration of Offshore Wind Power for a Steadier, Environmentally Friendlier, Supply of Electricity in China

Xi Lu

School of Engineering and Applied Sciences, Harvard University

Address: RM G2E, Pierce Hall, 29 Oxford St., MA 02138

Email: xilu@fas.harvard.edu

Phone: 617-960-6069

Michael B. McElroy (corresponding author)

School of Engineering and Applied Sciences and Department of Earth and Planetary Sciences, Harvard University

Address: 100C Pierce Hall, 29 Oxford St., MA 02138

Email: mbm@seas.harvard.edu

Phone: (617) 495-4359

Chris P. Nielsen

Harvard China Project and School of Engineering and Applied Sciences, Harvard University

Address: RM G2F, Pierce Hall, China Project, 29 Oxford Street, Cambridge, MA 02138

Email: nielsen2@fas.harvard.edu

Phone: 617-496-2378

Xinyu Chen

Department of Electrical Engineering, Tsinghua University

Address: RM 208, West main building, Tsinghua University, Beijing, 100084, China

Email: chenxinyu09@mails.tsinghua.edu.cn

Phone: +86 13466628985

Junling Huang

School of Engineering and Applied Sciences, Harvard University

Address: RM G2C, Pierce Hall, 29 Oxford St., MA 02138

Email: huang18@fas.harvard.edu

Abstract

Demand for electricity in China is concentrated to a significant extent in its coastal provinces. Opportunities for production of electricity by on-shore wind facilities are greatest however in the north and west of the country. Using high resolution wind data derived from the GEOS-5 assimilation, this study shows that investments in off-shore wind facilities in these spatially separated regions (Bohai-Bay or BHB, Yangtze-River Delta or YRD, Pearl-River Delta or PRD) could make an important contribution to overall regional demand for electricity in coastal China. An optimization analysis indicates that hour-to-hour variability of outputs from a combined system can be minimized by investing 24% of the power capacity in BHB, 30% in YRD and 47% in PRD. The analysis suggests that about 28% of the overall off-shore wind potential could be deployed as base load power replacing coal-fired system with benefits not only in terms of reductions in CO₂ emissions but also in terms of improvements in regional air quality. The interconnection of off-shore wind resources contemplated here could be facilitated by China's 12th-five-year plan to strengthen inter-connections between regional electric-power grids.

Key words

- Offshore Wind Power
- hour-to-hour variability
- firm capacity

1. Introduction

Production of electricity from wind power has expanded rapidly in China since 2006, with an annual growth rate of over 90% from 2006 to 2011. Total installed national capacity amounted to 62.7 giga-watts (GW) at the end of 2011. About 73.2 TWh of electricity was generated from wind in China in 2011, accounting for 1.6% of total electricity generation in the country (**Figure 1**) (SERC, 2012). Although almost all of the increase of wind power has come from development of land-based wind farms, offshore wind power in China has received increasing attention and is expected to expand significantly in the future. The first offshore wind project, consisting of 34 3-MW wind turbines (102 MW), was implemented at Shanghai Donghai Bridge in 2010. In the same year, four more offshore projects, including Binhai (300 MW), Sheyang (300 MW), Dafeng (200 MW) and Donghai (200 MW) successfully completed the first concession bidding process for offshore demonstration projects (Li et al., 2011). The successful bidding prices for these projects ranged from 0.62 RMB/kWh to 0.74 RMB/kWh, about 9.1 cents/kWh to 10.9 cents/kWh in 2010 US dollars. To ensure profitability, these projects benefit from a favorable concession policy, which guarantees higher bus-bar prices for electricity produced from offshore wind farms as compared with production from either onshore facilities or from conventional coal-fired power plants.

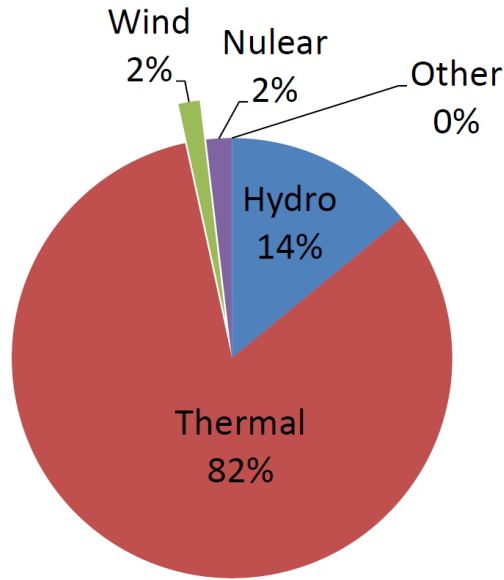


Figure 1. The electricity generation mix of China in 2011. Data derived from Chinese State Electricity Regulatory Commission

China's coal reserves and production are concentrated to the North and West of the country (particularly in Shanxi, Shaanxi and Inner Mongolia). To meet the increasing demand for energy in southeastern coastal provinces, where over 40% of the population is located (NBS, 2012), coal is first transported by rail east to the coast and shipped subsequently to the high demand centers in southeast. In 2010, 92% of coal consumed in Jiangsu province (responsible for the second highest GDP of all provinces in China) was imported from inland provinces. Rich onshore wind power resources tend also to be located to the North and West of China. To harvest this renewable source requires significant expansion of existing transmission grid system on a national scale. We shall argue here that investment in offshore wind resources would significantly reduce the demand for coal supply for the south, while providing at the same time a valuable low-carbon source of electric power.

The intrinsic variability of the output of power from individual wind farms poses a problem for integration at scale of this source into the existing power system. Production of electricity in coastal provinces of China is currently dominated by sources fueled by coal, with percentages ranging from 55% in Guangxi to as high as 91% in Shandong in 2010 (Ma et al., 2011). Coal-fired systems are relatively inflexible, with limited ramp-up and ramp-down capability to cope with the additional variations introduced by wind power. Direct or indirect electricity storage could help address this potential incompatibility. A number of pumped hydro power stations have already been built in China to cope with the increasing diurnal variability of load. Opportunities for further expansion of pumped storage are limited, however, due largely to constraints imposed by geography (compatible topography and hydrology). We shall argue that coupling outputs of wind farms from different regions of the Chinese coast could significantly offset the challenges associated with integrating this otherwise variable source.

The present analysis reports a statistical investigation of advantages that could be achieved in smoothing the variation of offshore wind power supply in the coastal areas of China through an optimal combination of power from geographically distributed offshore sites. A number of studies have examined the advantages of combining geographically distributed wind farms in the U.S. and Europe (Archer and Jacobson, 2007; Huang et al., 2013; Kempton et al., 2010). Kempton et al. (2010), analyzing five years of wind data from 11 meteorological stations distributed along the U.S. east coast, suggested that the output of wind power from an interconnected system there would be more reliable than that from any individual location. Archer and Jacobson (2007) explored the benefits of

connecting wind farms from up to 19 sites located in the U.S. Midwest, where annual average wind speeds at 80 m above ground exceeded 6.9 m/s. They found that an average of 33%, and a maximum of 47%, of yearly average wind power from interconnected farms could provide reliable, base-load electric power. Huang et al. (2013), using five years of hourly assimilated wind data, showed that the high-frequency variability of wind-generated power could be significantly reduced by coupling outputs from five to ten wind farms dispersed uniformly over ten states in the middle of the U.S. Their analysis suggests that more than 95% of the variability of the coupled system from this region was concentrated at time scales longer than a day, allowing operators of the overall system to take advantage of multiple-day weather forecasts in scheduling projected future contributions from wind.

Building on the earlier studies, the present analysis will focus on variations of hourly wind power from 12 offshore sites distributed along the Chinese coastline (see **Figure 2**), with a particular focus on the advantages that could be realized by coupling facilities distributed over three coastal economic zones (Bohai Bay, the Yangtze River Delta, and the Pearl River Delta). The total installed capacity for offshore wind power in China is projected to reach 30 GW in 2020 and 60 GW in 2030 (Wang et al., 2011). Most of the development plans for offshore wind power by the provincial governments are based primarily on considerations of the availability of local wind resources, with minimal attention to the challenges that would be associated with integration of this source into the existing power system. As will be shown here, these difficulties can be significantly mediated by adopting a more coordinated regional approach involving an

integration of wind resources for spatially separated coastal regions subject to important differences in prevailing meteorological conditions.

Section 2 summarizes the data and methods adopted for the present analysis. The variation of China's offshore wind resources, results of the optimization analysis, and related implications for the electric power systems of coastal regions in China are discussed in Section 3. Concluding remarks are presented in Section 4.

2. Data and Methods

Wind fields adopted for this analysis were derived for 2009 from the Goddard Earth Observing System Data Assimilation System (GEOS-5 DAS) by the U.S. National Aeronautics and Space Administration (NASA) (Rienecker et al., 2007). The data include records of wind activity on an hourly basis with a spatial resolution of 0.33 degree longitude by 0.25 degree latitude (approximately equivalent to 33 km \times 25 km at mid-latitude). Using the vertical profile of the power law described by Archer and Jacobson (2005), hourly wind speeds at 100 m are extrapolated from winds at 50 m and compiled for each grid cell in the database according to the relation

$$V(z) = V_{50} \left(\frac{z}{z_{50}} \right)^{\alpha}, \quad (1)$$

where V is the wind speed, z is the measurement height, and α indicates the friction coefficient (Archer and Jacobson, 2005; Masters, 2004), which varies as a function of the terrain where wind farms are located. A value of 1/7 is commonly assumed as a rough approximation for α in wind resource assessments. Here, we estimate the value of α for each hour for each grid cell of the GEOS-5 domain using equation (1), based on the wind

speeds at 10 m and 50 m available from this database. Both of these wind speed values are compiled through retrospective assimilation analysis, which takes account of spatial and temporal variations in surface roughness, as well as the stability of the atmosphere.

Wind power was computed for each hour using the power curve appropriate for GE 3.6 MW wind turbines (GE, 2006). This turbine model, specifically designed for operation in the offshore environment, has a rotor diameter of 111 m, and cutting-in, rated, and cutting-out wind speeds of 3.5 m/s, 14 m/s, and 27 m/s respectively. The ratios of real power outputs averaged hourly or annually to the rated capacity define respectively the hourly or annual capacity factors (CFs).

The spatial distribution of annual CFs for China's offshore wind resources is illustrated in **Figure 2**. Results are consistent with earlier assessments of offshore wind resources in China (Qin et al., 2010; Hong and Moller, 2011; Li et al., 2008; Lu et al., 2009; Jiang et al., 2013). In general, annual average CF values are found to be highest (>0.35) in the Taiwan Strait off the coast of Fujian, following by those for neighboring regions of Zhejiang to the north and Guangdong to the south. Offshore wind resources for Jiangsu, Shanghai, Shandong and Liaoning are also significant with CF values over the majority of offshore areas of these provinces equal to or greater than 0.25.

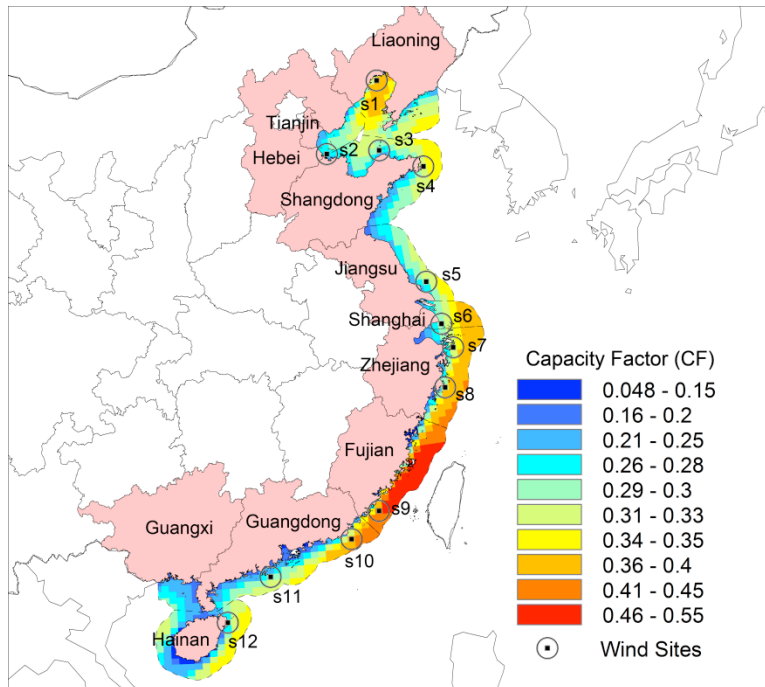


Figure 2. Distribution of annual average capacity factors (CFs) evaluated for deployment of a network of GE 3.6MW wind turbines within a distance of 80 km from the shoreline. The circled black dots indicate the locations of 12 sites considered in this analysis. Provinces and provincial-level municipalities with coastlines are in pink.

As illustrated in **Figure 2**, a total of 12 offshore sites were selected for purposes of this study, with sites 1 to 4 in the Bohai Bay region (hereafter referred to as BHB), sites 5-8 in the Yangtze River Delta area (YRD), and sites 9-12 in or near the Pearl River Delta (PRD). The BHB, YRD and PRD regions identify three of the most important economic zones and largest load centers in China. Several factors were taken into account in selecting these sites. First, all are located in regions where wind resources are relatively rich (with annual CFs at or above 0.25) and where, according to existing development plans, provincial governments are expected to exploit potentials for wind

power in the near future. The sites are also clustered in the three regions, to take advantage of heterogeneities in seasonal meteorological regimes across Chinese coastal regions, as discussed below. Second, the sites are geographically distributed over the coastal provinces with identical number of wind sites located in each economic zone. **Table 1** provides summary information on individual offshore sites in terms of locations, jurisdictions, affiliated coastal economic zones, and annual CFs estimated assuming installation of GE 3.6-MW turbines. In the present analysis, each offshore site was assumed to represent a hypothetical wind farm, each with the same installed capacity. This capacity was allowed to vary, depending on the total capacity evaluated for the combined system.

Table 1 The locations and annual capacity factors (CFs) for the 12 offshore sites selected in this analysis and average CFs of offshore sites within the economic zones

No.	Lon.	Lat.	Provinces/Municipalities	Site CFs	Zones	Zone CFs
s1	121.3	40.8	Liaoning (LN)	0.358	Baohai Bay (BHB)	0.298
s2	118.0	38.3	Hebei/Tianjin (HB+TJ)	0.259		
s3	120.7	38.0	Shandong (SD)	0.275		
s4	122.7	37.0	Shandong (SD)	0.301		
s5	121.7	32.5	Jiangsu (JS)	0.295	Yangtze River Delta (YRD)	0.306
s6	122.0	30.8	Shanghai (SH)	0.297		
s7	122.3	29.8	Zhejiang (ZJ)	0.308		
s8	121.7	28.3	Zhejiang (ZJ)	0.325		

s9	118.0	23.8	Fujian (FJ)	0.440	Pearl River Delta (PRD)	0.344
s10	116.7	22.8	Guangdong (GD)	0.279		
s11	113.0	21.5	Guangdong (GD)	0.278		
s12	111.0	19.8	Hainan (HN)	0.277		

3. Results and Discussion

3.1 China's Offshore Wind Power: Potential and Variation

Following the methodology introduced by Lu et al. (2009) and McElroy et al. (2009), the present study evaluates the potential of offshore wind resources for the coastal provinces of China subject to constraints imposed with respect to both water depth (≤ 30 m) and proximity to closest shoreline (≤ 80 km). Wind resources over such shallow, near-shore areas and intertidal zones are identified as the top priority for exploitation in China, since technologies for both turbines and foundations are mature and available for such deployment (Qin et al., 2010; Zhang et al., 2011). Regions characterized by CF values less than 0.2 were excluded for purposes of this study. The spacing between individual turbines in the hypothetical wind farms is taken as nine rotor diameters in the downwind direction, and five rotor diameters in the direction perpendicular to the prevailing wind ($9D \times 5D$). Overall power loss due to turbine-turbine interactions with this spacing estimated at about 10% (Kempton et al., 2007).

As summarized in **Figure 3**, consistent with earlier reports (Qin et al., 2010; Hong and Moller, 2011; Li et al., 2008; Lu et al., 2009; Jiang et al., 2013), this analysis suggests that wind energy over shallow-water regions could potentially supply a significant fraction of the total demand for electricity in the majority of China's coastal

provinces. The wind potentials in Tianjin, Hebei, and Guangxi provinces are insufficient to meet demands for these provinces or municipalities, due to relatively short coastlines and generally lower quality offshore resources. The aggregations of offshore wind potentials for the provinces or municipalities in BHB (LN, HB+TJ and SD), YRD (JS, SH and ZJ) and PRD (FJ, GD, HN and GX) zones are estimated at 781 TWh, 1134 TWh, and 1085 TWh respectively, potentials that may be compared with the corresponding zone-wide power demand of 838 TWh, 798 TWh and 652 TWh, respectively in 2010. On this basis, the availability of offshore wind is not considered to pose a serious constraint in the following analysis.

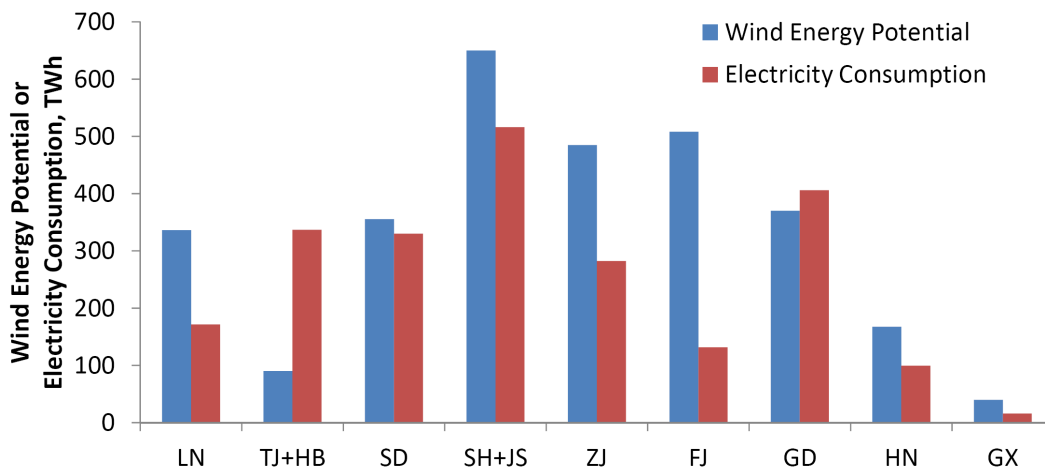


Figure 3 Offshore wind energy potentials for Chinese coastal provinces/municipalities in comparison with their demands for electricity in 2010. Abbreviations for the provinces/municipalities are defined in Table 1.

A temporal correlation analysis was conducted for all pairs of hourly CFs at the 12 offshore wind sites, in order to investigate the complementary effects of the temporal variations of offshore wind resources in different geographical locations. Resulting

correlation coefficients averaged for winter, spring, summer and fall are presented in **Figures 3a-3d** respectively. As illustrated in **Figure 4**, the correlation coefficients vary from -0.25 to 1 (the latter number reflecting the correlation of a site with itself). For all four seasons, hourly outputs of wind power from a specific site tend to correlate closely with those from adjacent sites. Correlation coefficients decrease with increasing separation of sites, consistent with findings in earlier studies (Archer and Jacobson, 2007; Huang et al., 2013; Kempton et al., 2010).

Pairs with highest correlations tend to be clustered in the three coastal zones as expected: s1-s4 in BHB, s5-s8 in YRD and s9-s12 in PRD. The cluster patterns exhibit clear seasonal differences, influenced most likely by the seasonality of large-scale weather patterns associated with the Southeast Asian monsoon. As illustrated in **Figure 4a**, hourly CFs from offshore sites within each coastal zone are relatively closely inter-correlated for the months of December, January and February. In winter, the upper-level westerly air flow is split and deflected by the Tibetan plateau, forming the subtropical jet anchored to the south and the polar-front jet to the north (Chang, 1971). The northern jet is more variable and weaker, influencing primarily wind conditions over Bohai Bay. As a result, the hourly wind power from the offshore sites within BHB (s1-s4) share similarities in terms of temporal variations, but in general they are poorly correlated with the wind power outputs from the offshore sites in the YRD and PRD zones. Winds from the YRD and PRD zones are influenced mainly by the southern subtropical jet stream. The covariance of wind sources from the YRD and PRD sites is interrupted, however, by the influence of the Taiwan Strait (evident particularly in the relatively weak correlation between adjacent sites s9 and s10).

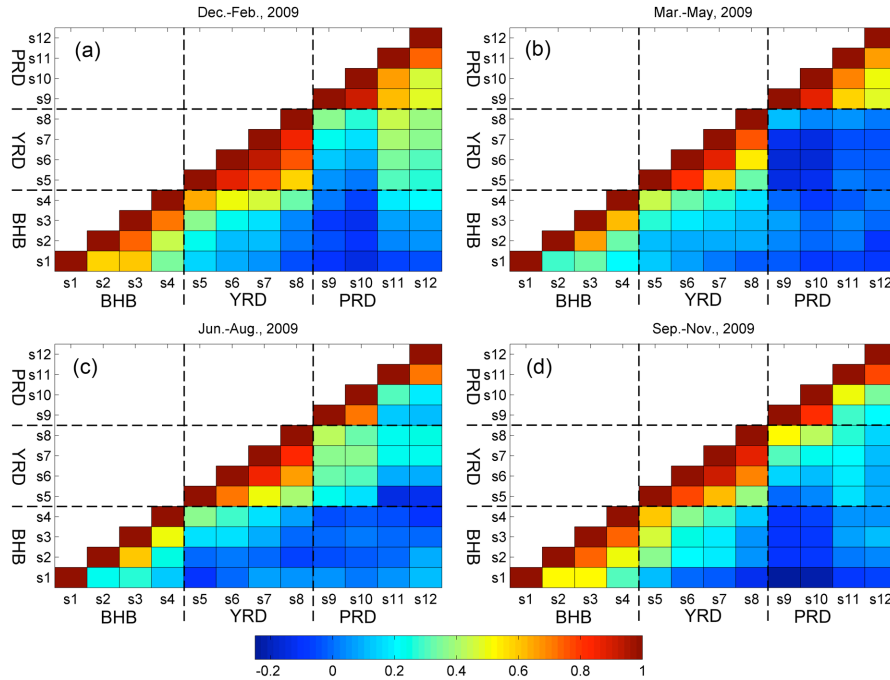


Figure 4 Correlation coefficients for hourly CFs for all pairs of the 12 offshore sites considered in this study: 3a shows results for winter (December, January and February); 3b for spring (March, April and May); 3c for summer (June, July and August); and 3d for fall (September, October and November).

As illustrated in **Figure 4c**, the correlation analysis for summer (Jun.-Aug.) indicates a pattern very different from that in winter. Offshore sites within YRD are influenced by the summer Pacific anticyclone to the east of China, and power outputs tend to be well correlated in this case. The correlation coefficients for offshore sites within either BHB or PRD show much weaker clustering, reflecting the greater complexity of weather systems over these two regions in summer. In spring (Mar.-May), temporal variations of wind power from offshore sites within YRD and PRD are

distinguished by clustered patterns (**Figure 4b**). Similar clustering is observed for BHB and YRD in fall (Sept. to Nov.) (**Figure 4d**).

3.2 Optimization Analysis

The results in **Figures 4a-4d** suggest that advantages could be realized by linking these regions. For any given hour, a low contribution of wind-generated power from sites in one coastal zone will be compensated often by a higher output from sites in another zone. If the 12 offshore sites in the three economic zones were all interconnected, the overall power output would be much less variable than the output from any individual site, and less variable than that for any individual zone. This raises the question as to how these zones could be optimally combined to reduce the overall variation of power output.

An optimization model was applied to determine the relative contributions of wind power from the BHB, YRD and PRD zones that would result in the lowest possible standard deviation of the hour-to-hour variation of power output from the combined system. The following objective function is designed to minimize the hour-to-hour variation of electricity produced by the interconnected sites, thus to ease the integration of wind power into the relatively inflexible, coal-dominated, existing electric power system:

$$Obj = \min \left(\sqrt{\frac{1}{N-1} \sum_{t=1}^{N-1} (\Delta CF_t - \overline{\Delta CF})^2} \right), \quad (2)$$

where ΔCF_t refers to the difference between the CFs for hour $t+1$ and for the previous hour. N is the total number of hours of a year, 8760 hours in this case of 2009. $\overline{\Delta CF}$ indicates the mean of hour-to-hour changes of CFs. Results are illustrated in **Figure 5**.

The contributions of wind power to the combined system from BHB, YRD and PRD are indicated by the scales on the three sides of the ternary plot, read in a counter-clockwise direction. The color scale indicates the corresponding values of the objective function for any combination of wind capacity shares from the three zones. The analysis suggests that the minimum standard deviation of hour-to-hour variation of wind power from the combined system would be achieved by allocating 24% of offshore capacity to the BHB area, 30% to the YRD area, and 47% to the PRD area. Should China elect to exploit this distribution of sites to add 60 GW of offshore wind farms in 2030 as projected, the analysis implies that this could be achieved by installing 14 GW in the BHB zone, 18 GW in the YRD zone, and 28 GW in the PRD zone. This combination would provide the best, steadiest, overall, power output.

It should be emphasized, as indicated earlier, that current plans have not as yet sought to exploit the advantages that could be achieved from a targeted coupling of separate wind farms. Present development plans for offshore wind power emphasize the YRD area (Qin et al., 2010). In addition, a wind base in Jiangsu Province (included in our PRD region), consisting mainly of offshore wind farms and with a total capacity larger than 10 GW, is proposed for completion by 2020. Offshore wind development plans for PRD by comparison are much more modest.

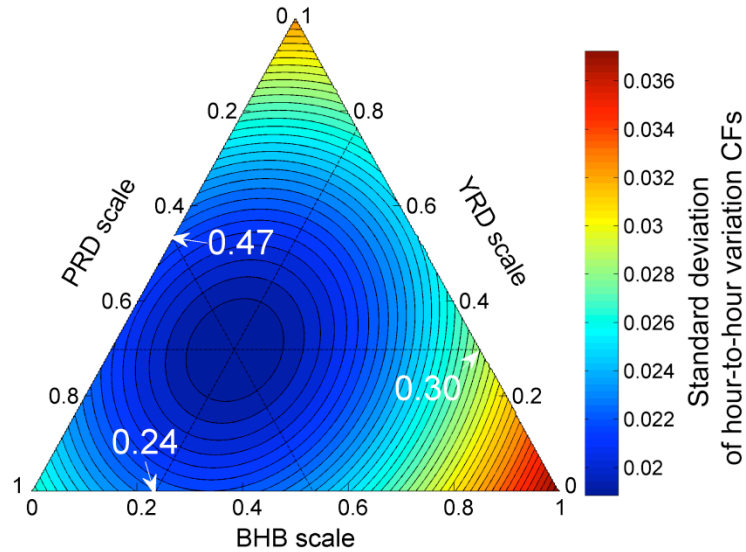


Figure 5 Optimization of the Combined Offshore System from the Bohai Bay (BHB), Yangtze River Delta (YRD) and Pearl River Delta (PRD) zones. Values on the arrows indicate the optimal shares of capacity for offshore wind power installations for the three selected individual zones.

3.3 Implications to the Electric Power System

The histograms in **Figure 6** offer a different perspective on the value of the optimization, as reflected in the frequency distributions of hour-to-hour variations of CFs over the course of 2009. The histogram in the top left panel for a single site (s3) indicates minimal change in CF on an hour-to-hour basis for approximately a quarter of the time (more than 2000 hours out of 8760). Hour-to-hour changes in CF in excess of 0.05 (i.e. from 0.38 to more than 0.43 or less than 0.33) are projected to occur for approximately 1925 hours over course of the year.

Figure 6 includes a summary of data on hour-to-hour variations in CF for selected sites from each of the three zones (s3, s7 and s11) together with results for the interconnected composite. The combined system clearly reduces the range of high

frequency variability: the frequency distribution is narrowed significantly. Over the course of the year, the largest hour-to-hour increase in CF predicted for any one of the three selected sites was 0.85 (at s11): the largest decrease was 0.44 (at s7). If the capacity of wind farms installed at these individual sites amounted to 100 MW, this would imply that power outputs could increase 85 MW, or decrease by 44 MW from one hour to the next. In the case of the coupled system with capacity of 100 MW in total, hour-to-hour changes would be significantly reduced, ranging from as little as -7 MW to +15 MW. What this means is that the need for quick-ramping capacity to compensate for variability in the supply from offshore wind resources would be significantly reduced with the combined system as compared to the situation that would apply in the absence of interconnection.

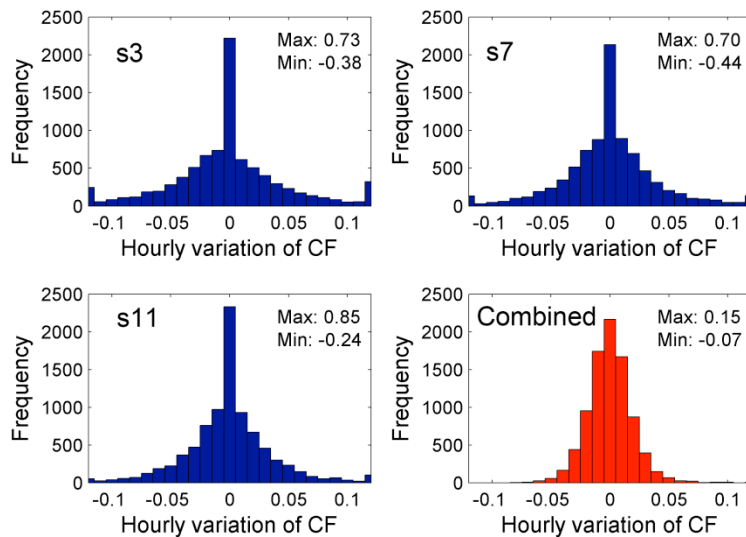


Figure 6 Hour-to-hour variations of CFs for the offshore sites s3, s7, and s11, and for the optimally combined system. The scale on the vertical axes indicates the number of hours out of 8760 hours of one year as represented by a given variation of CF.

The frequency distributions of hourly CFs (as opposed to hour-to-hour changes in CF) over the course of 2009 for the same three offshore sites and for the optimally combined system are illustrated in **Figure 7**. The distribution of CF values for the combined system is significantly more concentrated (much less variable) than that for any individual offshore site. The variability of power outputs from a single site is evidenced by the wider distribution of CF values, varying from 0 to 1, with large probabilities at the two extremes. In contrast, the frequency spectrum of CFs for the optimally integrated system exhibits a Rayleigh distribution, which a peak at 0.25 combined with a broad tail extending to higher values. **Figure 7** suggests that the intermittency of wind power (referring to occasions of zero power output) can be effectively eliminated in the optimally combined case. Similar results were found in earlier studies of both onshore and offshore wind sources in the U.S. (Huang et al., 2013; Kempton et al., 2010). The standard deviation (σ_{CF}) of the hourly CFs for the optimally combined system was found to decrease to 0.18, a value corresponding to approximately half of that for the individual sites s3 (0.30), s7 (0.30) and s11 (0.28).

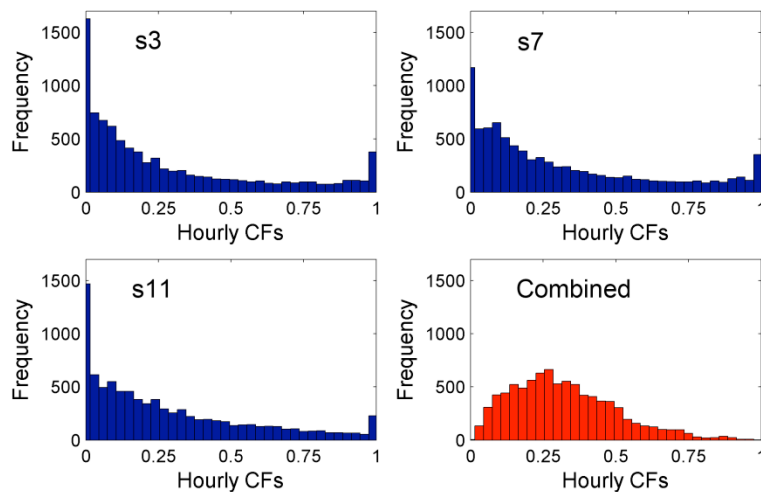


Figure 7 Frequency distribution of CFs over the course of the year (2009) for offshore sites s3, s7, s11, and for the optimally combined system. The scale of the vertical axes indicates the number of hours out of 8760 hours of one year corresponding to particular values of CF.

Generation duration curves, which order the hourly power outputs or CFs from highest to lowest values over the entire year of 8760 hours (Masters, 2004) provide a useful tool for evaluating the reliability of electric power from renewable sources, including wind and solar. Duration curves for the three offshore sites and for the optimally combined system are presented in **Figure 8**. The area under each curve in the figure defines the total electricity generated per unit of installed capacity. **Figure 8** illustrates thus the number of hours per year that an individual offshore site or combined system could realize a CF greater than any particular value. As indicated, CFs for the individual offshore sites exhibit either high or low extremes for a significant number of hours per year. For s7, for example, the results indicate that this site would fail to produce any electricity (CF=0) for 989 hours of the year, 11.3% of the time. On the other hand, the site would produce maximum power (CF=1) for 294 hours, 3.4% of the time. The generation duration curve of the optimally combined system is flatter than that for any of the individual sites.

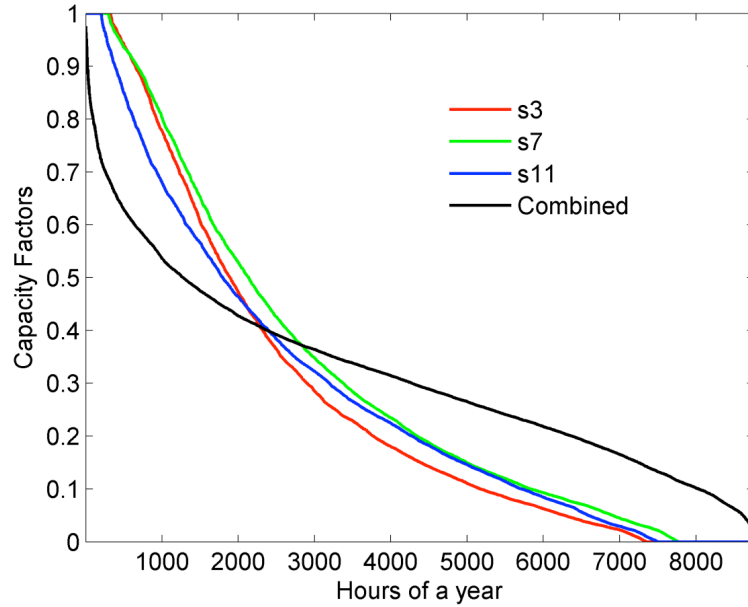


Figure 8 Generation duration curves for the offshore sites s3, s7, s11 and for the optimally combined system.

Another way to quantify the benefit of the combined system is to focus on the increase in the firm capacity of wind power, defined as the fraction of installed capacity that remains online with the same probability as that for a coal-fired power plant (Archer and Jacobson, 2007). Coal-fired plants in China are offline from 5.6% to 14.7% of the time, for an average of 7.6%, in order to allow for both scheduled and unscheduled maintenance, and forced outage (EPRMC, 2010-2012). To accommodate an equivalent available factor (EAF) for wind compared to coal-fired plants (92.4%), wind systems should be operational for at least 8094 hours of the year. The limiting CF value corresponding to this condition is equal to 0.092 as indicated in **Figure 8**. The firm capacity of the optimally combined system corresponds therefore to about 9.2% of the total installed capacity. The power output consistent with this firm capacity requirement

accounts thus for 27.9% of the total power generated from the combined system over the entire year, implying that power of this magnitude from the combined system could serve as base load reducing accordingly the demand for power from coal-fired plants.

Figure 9 illustrates the hourly CFs for s7 and for the optimally combined system for each of the four seasons, including comparison with the seasonal limiting values of CF for the combined system as subjected to the same requirements of EAF (92.4%) as for the coal-fired plants. The power output from the combined system is clearly less variable than that from s7 over all four seasons. As indicated in the figure, in the absence of interconnection, the firm capacity available from individual plants such as s7 is relatively small. As a result, power outputs from individual wind farms are conventionally treated as negative load. In contrast, the firm CFs from the combined system in winter can be as great as 0.126 and ever larger in spring (0.134) and fall (0.143), corresponding to 33.3%, 41.5% and 37.8% of total power generated using wind for these seasons. The firm CF of the interconnected system is significantly lower in summer (0.055), reflecting primarily the lower quality of wind resources during this season. The deficit could be made up in this case however by taking advantage of the increased availability of power from hydro facilities, particularly in the southeastern region, in that season.

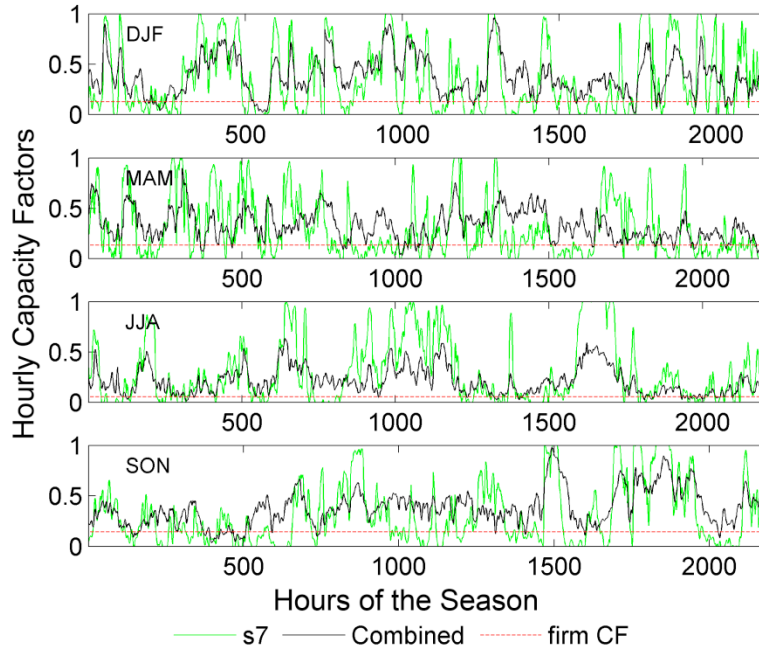


Figure 9 Hourly CFs for s7 and for the optimally combined system for four seasons of 2009: DJF (Dec.-Feb.), MAM (Mar.-May), JJA (Jun.-Aug.) and SON (Sept.-Nov.). The dashed red line indicates the corresponding firm capacity factors for the combined system for each season.

4. Concluding Remarks

An optimization model was adopted to explore the complimentary qualities of wind power from 12 offshore sites distributed over three coastal economic zones (BHB, YRD, and PRD) in China. The analysis was based on wind data derived from GEOS-5 assimilated meteorological fields. The spatial distribution of annual CFs for shallow-sea areas of coastal zones in China, evaluated using GEOS-5 winds, is consistent with earlier assessments (Qin et al., 2010; Lu et al., 2009; McElroy et al., 2009; Xiao et al., 2010; Jiang et al., 2013). Correlation analyses for the 12 offshore sites indicate that hourly wind power outputs (expressed in CFs) from the three coastal zones are weakly correlated, thus

complementary in terms of the ability of an integrated system to reduce temporal variability. An optimal combination of wind power from these coastal zones (24% from BHB, 30% from YRD, and 47% from PRD) was found to minimize hour-to-hour variation of the overall power output. The decrease in hour-to-hour variations from wind power reduces the requirement for quick-ramping capacity in the power system as needed to compensate for variability introduced by offshore wind. The results of the optimization have important implications for planning of future developments for offshore wind resources in China. Should China elect to invest in 60 GW of offshore wind facilities by 2030, the present analysis suggests that 14 GW of this investment should be allocated within BHB, 18 GW within YRD, and 28 within PRD. This combination would ensure maximum reliability of the power supply from an interconnected offshore wind system.

The frequency distribution of the hourly CFs of the optimally combined system is concentrated in a CF range of 0.15 to 0.50. Intermittency is effectively eliminated in this case. The optimally combined system can supply 9.2% of its total capacity as firm capacity, which guarantees reliable power output with an offline record of no more than 7.6%, equivalent to the conditions realized by existing coal-fired power plants in China. Over the course of a year, about 27.9% of the power generated from the optimally combined system could be deployed as base load, replacing potentially in this case the demand for power production by coal-fired systems.

To realize the advantage of the steadier electricity supply from offshore wind identified in this study, it will be necessary to invest in a significant expansion of the existing transmission grid system, to interconnect the wind facilities contemplated for the three regions identified here. Kempton et al., (2010) proposed an offshore transmission

cable to link potential wind farms along the U.S. eastern coast in order to mitigate the variations of overall anticipated power output. An “Atlantic Independent System Operator” was specifically suggested by Kempton et al., (2010) to manage and regulate the market for offshore wind power off the east coast of the US. China, however, may be expected to follow a different path in developing its off-shore resources. The likely strategy in this case may be expected to involve enhancing interconnectivity of the land-based regional grid systems. Wind resources from the BHB, YRD and PRD development sites are likely to be integrated directly into the North China, East China, and South China regional grids respectively. The capacities to exchange electricity among these three grids, however, are currently limited. An element of China’s 2011-2015 12th Five-Year Plan (Wang et al., 2011; Li, 2009) proposes construction of a super grid system using ultra high voltage alternative current (AC) lines integrating the North China, Central China, and Eastern China regional grids into a super grid system. This would be connected in turn to the Northeast, Northwest, and South China grids through direct current (DC) lines, facilitating opportunities for interconnection of the geographically distributed offshore wind resources highlighted in this study.

Acknowledgement

This research was supported by the National Science Foundation, Grant AGS-1019134. We thank two anonymous reviewers for helpful comments and suggestions.

References

1. Archer, C.L., Jacobson, M.Z., 2005. Evaluation of global wind power. *J. Geophys. Res.* 110, D12110.
2. Archer, C.L., Jacobson, M.Z., 2007. Supplying Baseload Power and Reducing Transmission Requirements by Interconnecting Wind Farms. *J. Appl. Meteor. Climatol.* 46, 1701-1717.
3. Chang, J.-H., 1971. The Chinese Monsoon. *Geographical Review* 61, 370-395
4. GE, 2006. 3.6 MW Wind Turbine Technical Specifications, in: Energy, G. (Ed.). General Electric Energy, Fairfield, Connecticut.
5. EPRMC, 2010-2012. General report on power reliability for the first half years of 2010, 2011 and 2012, Electrical Power Reliability Management Center, State Electricity Regulatory Commission, Beijing, China.
6. Qin, H., Liu, M., Wang, Y., Zhao, J., Zeng, X., 2010. China: An Emerging Offshore Wind Development Hotspot With a new assessment of China's offshore wind potential, in: Reinvang, R., Enslow, R., Beaumont, H. (Eds.). WWF, CWEA and Sun-Yet-Sen University, Beijing, China, p. 64.
7. Hong, L.X., Moller, B., 2011. Offshore wind energy potential in China: Under technical, spatial and economic constraints. *Energy* 36, 4482-4491.
8. Huang, J., Lu, X., McElroy, M.B., 2013. The meteorology of wind energy in the US and its implication on the interconnection of wind farms. *Renewable Energy*, accepted.

9. Jiang, D., Zhuang, D., Huang, Y., Wang, J., Fu, J., 2013. Evaluating the spatio-temporal variation of China's offshore wind resources based on remotely sensed wind field data. *Renewable and Sustainable Energy Reviews* 24, 7.
10. Kempton, W., Archer, C.L., Dhanju, A., Garvine, R.W., Jacobson, M.Z., 2007. Large CO₂ reductions via offshore wind power matched to inherent storage in energy end-uses. *Geophys. Res. Lett.* 34, 5.
11. Kempton, W., Pimenta, F.M., Veron, D.E., Colle, B.A., 2010. Electric power from offshore wind via synoptic-scale interconnection. *Proc. Natl. Acad. Sci. USA* 107, 7240-7245.
12. Li, J., 2009. From Strong to Smart: the Chinese Smart Grid and its relation with the Globe. *Asia Energy Platform*, Hong Kong p. 10.
13. Li, J., Gao, H., Wang, Z., Ma, L., Dong, L., 2008. *China Wind Power Report 2008*. China Environmental Science Press, Beijing, China.
14. Li, J., Shi, P., Gao, H., 2011. *China Wind Power Outlook 2010*. Chinese Renewable Energy Industries Association, Beijing, p. 108.
15. Lu, X., McElroy, M.B., Kiviluoma, J., 2009. Global potential for wind-generated electricity. *Proc. Natl. Acad. Sci. USA* 106, 10933-10938.
16. Ma, J., Zhang, W., Luo, L., Xu, Y., Xie, H., Xu, X., Li, Q., Zheng, J., Sheng, L. (Eds.), 2011. *China Energy Statistical Yearbook 2011*. China Statistics Press, Beijing.
17. Masters, G.M., 2004. *Renewable and Efficient Electric Power Systems*. A John Wiley & Sons, Inc., Hoboken, New Jersey.

18. McElroy, M.B., Lu, X., Nielsen, C.P., Wang, Y., 2009. Potential for Wind-Generated Electricity in China. *Science* 325, 1378-1380.
19. NBS, 2012. Tabulation on the 2010 Population Census of People's Republic of China. China Statistics Press, Beijing.
20. Rienecker, M.M., Suarez, M.J., Todling, R., Bacmeister, J., Takacs, L., Liu, H.-C., Gu, W., Sienkiewicz, M., Koster, R.D., Gelaro, R., Stajner, I., Nielsen, J.E., 2007. The GEOS-5 Data Assimilation System-Documentation of Versions 5.0.1, 5.1.0, and 5.2.0., in: Suarez, M.J. (Ed.), Technical Report Series on Global Modeling and Data Assimilation. NASA, Washington, DC, p. 118.
21. SERC, 2012. China Power Regulation Annual Report 2011. State Electricity Regulatory Commission, Beijing, p. 111.
22. Xiao, Z., Zhu, R., Song, L., Cheng, X., He, X., Jiang, Y., Lin, S., Liu, Y., Shen, Y., Tao, S., Wang, X., Wang, Y., Xu, J., Yuan, C., Zhang, D., Zhang, X., Zhang, Y., Zhao, D., Zhou, R., Zhu, J., 2010. Assessment of Wind Resources in China 2009, 1 ed. China Meteorological Press, Beijing, China.
23. Zhang, D., Zhang, X.L., He, J.K., Chai, Q.M., 2011. Offshore wind energy development in China: Current status and future perspective. *Renew. Sust. Energ. Rev.* 15, 4673-4684.
24. Wang, Z., Shi, J., Zhao, Y., 2011. Technology Roadmap: China Wind Energy Development Roadmap 2050. International Energy Agency and Energy Research Institute, Paris, France, p. 56.